



## MECE09033 2025: Optimised Solar Still

Group 6

September - November 2025

### GitHub Repository URL:

<https://github.com/JINXUANPAN/Computational-methods-and-modelling-3.git>

### Contributions of each Team Member:

<b>Abby Birchall</b> s2622777	<ul style="list-style-type: none"><li>• System Overview</li><li>• ODE Solver</li><li>• Root finding</li></ul>
<b>Matias Lander</b> s2574648	<ul style="list-style-type: none"><li>• Mathematical Modelling</li><li>• Design Analysis</li><li>• Conclusions</li></ul>
<b>Sandy Wedderburg</b> s2544622	<ul style="list-style-type: none"><li>• Solar Irradiance forcer</li><li>• READ ME file</li><li>• Regression Model</li></ul>
<b>Jinxuan Pan</b> s2495161	<ul style="list-style-type: none"><li>• Regression Model</li><li>• ODE solver</li><li>• Mathematical Modelling</li></ul>
<b>Campbell Graham</b> s2544188	<ul style="list-style-type: none"><li>• Introduction</li><li>• System Overview</li><li>• Conclusions</li></ul>

### Summary of Group Work:

Collaborative work was consistently maintained throughout the assignment. Early in the project, we divided tasks based on individual strengths: those more confident in coding focused on implementation and testing, while those with stronger writing skills took responsibility for developing the report. This ensured that each member contributed effectively while also allowing opportunities for others to learn by observing different stages of the workflow.

We used several collaborative tools to stay organised and maintain transparency. GitHub was central to our coding process: each member worked on their own branch, created pull requests, and had their work reviewed by another teammate before merging into the main branch. This peer-review system not only improved code quality but also helped us learn from one another's approaches. We also used a shared Gantt chart to track deadlines and monitor progress, and Trello to visualise task allocation across lists such as 'To Do', 'In Progress', 'Needs Review', and 'Completed'.

Communication was maintained through bi-weekly external meetings, which were essential for realigning priorities, resolving uncertainties, and ensuring the project remained on track. Outside these meetings, we primarily used Teams to provide updates or request support when challenges arose.

While we encountered some practical issues related to coding logistics (e.g. unfamiliarity with GitHub, lack of necessary relevant data, etc), these were resolved collaboratively by discussing alternative solutions and reviewing each other's work. Additionally, we occasionally engaged in informal pair programming sessions, which helped clarify complex logic and strengthened our collective problem-solving skills as well. Overall, the group worked cohesively, supported each other's learning, and maintained a consistently productive workflow.

- Teams Collaboration: 33 Posts, 76 Replies, 56 Reactions, 42 Mentions
- Shared Gantt chart, outlining internal deadlines [see 'Docs' file]
- Shared Trello Board (Used for real-time task allocation and tracking): CMM3 Group 6 Progress Tracker
- GitHub: 38 commits within last 28 days

# Contents

<b>1</b>	<b>Introduction</b>	<b>1</b>
<b>2</b>	<b>System Overview</b>	<b>1</b>
<b>3</b>	<b>Mathematical Modelling and Numerical Methods</b>	<b>2</b>
3.1	Overview . . . . .	2
3.2	Solar Irradiance Reconstruction and Regression . . . . .	2
3.3	System Modelling and ODE Formulation . . . . .	2
3.4	Numerical Implementation . . . . .	3
3.5	Root Finding: Area Optimisation . . . . .	3
3.6	Summary of Numerical Methods . . . . .	4
3.7	Assumption Validation . . . . .	4
<b>4</b>	<b>Design Analysis</b>	<b>4</b>
4.1	Comparison with Literature and Expected Performance . . . . .	4
4.2	Irradiance Distribution and Regression Fit . . . . .	4
4.3	Thermal Response and Freshwater Output . . . . .	5
4.4	Basin Area Optimisation and Root-Finding . . . . .	5
4.5	Sanity Checks and Physical Plausibility . . . . .	6
4.6	Summary . . . . .	6
<b>5</b>	<b>Conclusions</b>	<b>6</b>

# 1 Introduction

Over 97% of the Earth's water is saltwater [1], and with 2.1 billion people across the planet still without access to safely managed drinking water [2], desalination via solar stills could provide a solution to households faced with this issue.

We wanted our project scope to analyse and assess a possible solution to a real-world problem whilst involving our interests in certain principles such as thermodynamics and environmental engineering. Our aim is to use mathematical modelling and numerical analysis of the desalination process to find the minimum basin area required to accumulate the volume of potable water that the average household needs per day.

Wanting our solution to be as realistic and relevant as possible, we took time to consider solar irradiance data, realistic access to saltwater and need for potable water solutions in deciding a target location. We decided to use data from Algeria to carry out this project; however, it is also important to note that we aimed to make our methods repeatable such that they can be reapplied to any relevant location with those in need of a reliable drinking water solution.

## 2 System Overview

The system investigated in this study is a **single-slope passive solar still**, designed to convert saline water into potable water using solar energy. The still comprises a **black-painted aluminium basin** covered by a **4 mm thick transparent glass plate** inclined at **23°**. A **shallow 20 mm layer** of saline water is maintained in the basin, and all joints are sealed with **silicon rubber** to prevent vapour leakage. Condensed water is collected in a **semi-cylindrical distillate trough** positioned along the lower edge of the glass and directed to a storage vessel.

During operation, **solar radiation is transmitted through the glass cover and absorbed by the basin surface**, heating the water and initiating **evaporation**. The vapour condenses on the cooler inner surface of the glass, releasing latent heat and forming droplets that flow downward into the outlet.

System performance depends primarily on **solar insolation, thermal losses, and basin area**. In this project, the **basin area is optimised** to achieve the required daily distillate yield.

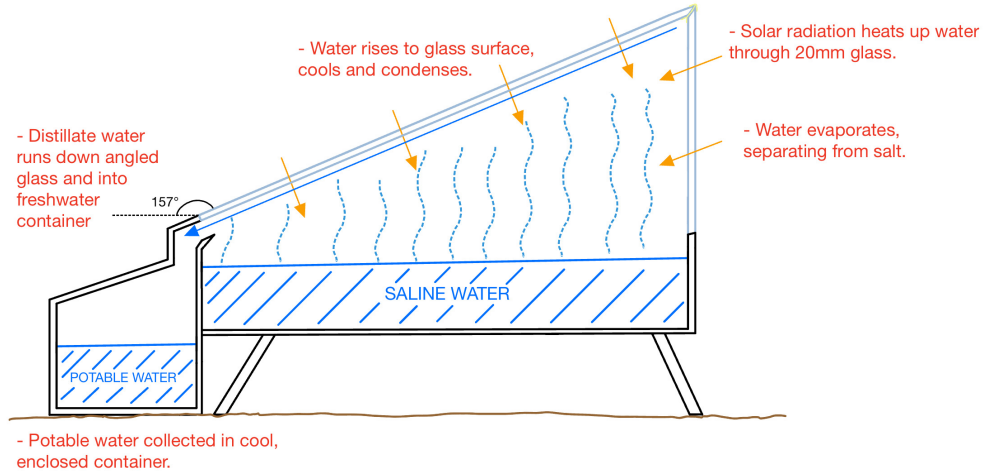


Figure 1: Solar Still Diagram

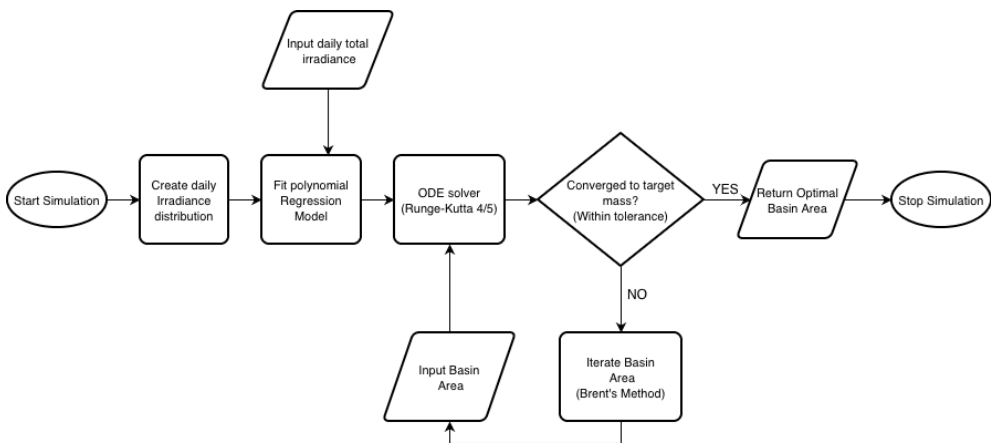


Figure 2: Flow diagram of modelled system

### 3 Mathematical Modelling and Numerical Methods

#### 3.1 Overview

This model simulates the transient thermal behaviour and freshwater production of a single-basin solar still. It predicts the water and glass temperatures over a 24-hour cycle and computes the total condensed water mass. The model integrates three numerical techniques: polynomial regression to construct a continuous irradiance input, Runge–Kutta integration to solve coupled energy balances, and Brent root-finding to optimise the basin area for a target yield.

#### 3.2 Solar Irradiance Reconstruction and Regression

A significant challenge was the lack of historical hourly irradiance data for Algeria. Only daily totals were available, so an “*irradiance forcer*” was created using a 15-day hourly forecast dataset.

The system was modelled using a Total Daily Irradiance of 4600 Wh/m<sup>2</sup> representative of the Direct Normal Irradiance in the Algiers region, over period 1994-2018 [3]

The average proportion of total daily irradiance occurring in each hour (e.g., 11.5% at 15:00) was used to distribute daily totals into hourly values:

$$G_h = f_h G_{\text{daily}}, \quad (1)$$

where  $f_h$  is the hourly fraction. This reconstructed dataset was then fitted using a **cubic polynomial regression**,

$$G(t) = a_3 t^3 + a_2 t^2 + a_1 t + a_0, \quad (2)$$

which provides a smooth, continuous irradiance function usable by the ODE solver, which is reliant on the differentiable nature of the function. The cubic form captures the asymmetric shape of irradiance throughout the day, rising sharply in the morning, peaking at noon, and tapering off in the evening, without over-fitting.

Comparably, Spline Interpolation was not opted for, due to large gaps between data points. Measuring one data point per hour, this numerical method is vulnerable to overshooting or oscillation between peaks, which would not be representative of the trend in irradiance throughout the day. Furthering this, higher-order polynomials were not used due to Runge’s phenomenon, which causes extreme oscillation at the edges of the domain. Together, these factors made a cubic regression model the most dependable and physically representative way to model the irradiance curve for use in the thermal simulation.

#### 3.3 System Modelling and ODE Formulation

The solar still is idealised as two interacting thermal nodes: basin water ( $T_w$ ) and glass cover ( $T_g$ ), exchanging heat by convection, radiation, and evaporation. Key assumptions are:

- Lumped-body model for both nodes (uniform temperature distribution).
- Constant material and environmental properties.
- Perfect basin insulation and 80% vapor condensation efficiency ( $\eta_{\text{coll}} = 0.8$ ), accounting for system losses.

Applying energy conservation gives the coupled ODEs:

$$M_w C_w \frac{dT_w}{dt} = (I(t) \cdot \tau_g \cdot A) - Q_{\text{evap}} - Q_{r,w-g} - Q_{c,w-g} - \dot{m} C_w T_w \quad (3)$$

$$M_g C_g \frac{dT_g}{dt} = (I(t) \cdot \alpha_g \cdot A) + Q_{\text{evap}} + Q_{r,w-g} + Q_{c,w-g} - Q_{r,g-\text{sky}} \quad (4)$$

where:

- $I(t)$ : Solar insolation (W/m<sup>2</sup>)
- $A$ : Basin area (m<sup>2</sup>)
- $\tau_g$ : Transmittance of glass
- $\alpha_g$ : Absorptivity of glass
- $Q_{\text{evap}}$ : Evaporative heat transfer from water to glass (W)
- $Q_{r,w-g}$ : Radiative heat transfer from water to glass (W)
- $Q_{c,w-g}$ : Convective heat transfer from water to glass (W)
- $Q_{r,g-\text{sky}}$ : Radiative heat transfer from glass to sky (W)
- $\dot{m}$ : Instantaneous mass flow rate of evaporated water (kg/s)

The evaporative heat transfer is given by:

$$Q_{\text{evap}} = h_{e,w-g} A (T_w - T_g)$$

where  $h_{e,w-g}$  is the evaporative heat transfer coefficient.

The radiative and convective heat transfer rates are calculated as:

$$Q_{r,w-g} = h_{r,w-g} A (T_w - T_g), \quad Q_{c,w-g} = h_{c,w-g} A (T_w - T_g)$$

The radiative heat transfer to the sky is modelled as:

$$Q_{r,g-\text{sky}} = \varepsilon_g \sigma A (T_g^4 - T_{\text{sky}}^4)$$

The evaporation rate is calculated as:

$$\dot{m} = \frac{h_{e,w-g} A (T_w - T_g)}{h_{fg}} \quad (\text{kg/s})$$

where  $h_{fg}$  is the latent heat of vaporisation.

The collected water mass evolves as:

$$\frac{dM_{\text{col}}}{dt} = \eta_{\text{coll}} \cdot \dot{m}$$

### 3.4 Numerical Implementation

The above system was solved in Python using `scipy.integrate.solve_ivp` with the **Runge–Kutta 4/5 (RK45) method**. Initial conditions were:

$$T_w(0) = 303 \text{ K}, \quad T_g(0) = 298 \text{ K}, \quad M_{\text{col}}(0) = 0.$$

The simulation outputs water and glass temperature profiles, instantaneous evaporation rates, and cumulative daily freshwater yield.

This adaptive solver offers high accuracy for smooth, non-stiff systems by automatically adjusting the timestep as conditions change: resolution is increased during rapid temperature variations (e.g. midday), while larger steps are taken as the system evolves more slowly (e.g. early morning). This ensures an effective balance between stability and computational cost. Because evaporation is highly sensitive to the temperature differences between the water and glass, such fine-scale accuracy is essential to avoid amplifying errors in the predicted evaporative flux.

The balance between accuracy and computational cost is central to choosing an ODE solver. A forward Euler scheme would require extremely small timesteps to remain stable, drastically increasing computation time. Higher-order Runge-Kutta methods provide adaptive stepping, but the gain in accuracy does not justify their additional cost for this system. Likewise, stiff-solvers, such as backward Euler, were rejected because the system is not strongly stiff, making their iterative nonlinear solves unnecessarily expensive.

### 3.5 Root Finding: Area Optimisation

The system was modelled using a potable water target of **24 Kg per day**, sufficient for two households, each consisting of four people, with this upper limit chosen to reflect Algerian climate conditions [4].

The Basin Area required to meet the daily potable water demand is obtained using the `brentq` root-finding algorithm (located within the `scipy.optimize` package) which locates a root via a change of sign of two output values. Two basin-area values that generate outputs of opposite sign are first identified to bracket the solution. Brent's method then refines this interval using a combination of the highly reliable bisection method, and a faster interpolation step (e.g. secant). The algorithm automatically selects the safest valid option at each iteration, ensuring rapid and stable convergence.

Operationally, the model begins with a basin area of  $1 \text{ m}^2$ , before computing the daily water production and iteratively adjusting the area until the predicted output satisfies the required demand within the specified tolerance. The operational logic of the `brentq` algorithm is summarised below:

---

#### Algorithm 1 Brentq Method (Simplified)

---

- 1: **Input:**  $a, b$  such that  $f(a)$  and  $f(b)$  have opposite signs
  - 2: **while** not within tolerance **do**
  - 3:     Compute interpolation estimate (secant or inverse quadratic)
  - 4:     **if** estimate is valid **then**
  - 5:         Accept interpolation step
  - 6:     **else**
  - 7:         Perform bisection step
  - 8:     **end if**
  - 9:     Update interval to keep root bracketed
  - 10: **end while**
  - 11: **Return** root estimate
- 

For the optimised solar still area to be determined, a full simulation of the ODE system is required for each candidate value of Area. This is extremely computationally expensive, which is why efficiency is prioritised. Brent's method converges in very few iterations, minimising the number of simulations needed and therefore forming a key justification for its use.

Comparably, the Newton-Raphson method requires the derivative of the production function, which is unreliable to approximate numerically, since each evaluation involves solving a full set of ODEs, making it unsuitable for this system. The secant method avoids derivatives but is highly sensitive to initial guesses and provides no guarantee for convergence, which is problematic when each evaluation is computationally expensive. The bisection method is extremely robust but

would require many costly iterations if used alone. Brent's method overcomes these shortcomings outlined by combining bisection's robustness with the speed of interpolation-based steps, ensuring reliable and efficient convergence for this application.

### 3.6 Summary of Numerical Methods

- **Regression:** Created a continuous polynomial function  $G(t)$  from hourly irradiance data to provide a realistic solar input.
- **ODE Solving:** Applied RK45 integration to determine  $T_w(t)$ ,  $T_g(t)$ , and  $M_{col}(t)$  through time-dependent heat and mass balances.
- **Root-Finding:** Iteratively adjusts basin area  $A$  to achieve a desired daily output (described in a separate section).

### 3.7 Assumption Validation

Model assumptions are justified by the system's scale and operation. A lumped thermal model is valid since conduction through a 3 cm water layer occurs rapidly relative to hourly heating. Constant properties are acceptable for the narrow temperature range (25–70°C). An 80% condensation efficiency was used to account for non-ideal recovery (e.g. incomplete condensation and operational losses); 100% efficiency would be unrealistic and inconsistent with observed solar still performance. Sensitivity checks confirmed that key results, such as peak temperature and total yield, vary linearly with minor parameter deviations, indicating numerical robustness.

## 4 Design Analysis

This section presents the analysis of the solar still model, focusing on the performance of the irradiance reconstruction, thermal response, freshwater yield, and basin area optimisation. The objective is to assess whether the system behaves in a physically realistic manner and to verify that model outputs satisfy the engineering sanity checks defined earlier. The discussion begins by comparing our simulated performance with values reported in the literature to establish external validity before examining the behaviour of each subsystem in detail.

### 4.1 Comparison with Literature and Expected Performance

The results produced by the model demonstrate strong agreement with experimentally verified behaviour of single-basin passive solar stills. Using a representative daily solar profile for the Algiers region, the model was run over a 10-hour daylight window, during which evaporation naturally occurs under typical irradiance conditions. The predicted temperatures reached approximately 65 °C for the basin water and 55 °C for the glass cover, values that fall squarely within the temperature ranges commonly observed in laboratory and field measurements.

The corresponding simulated daily freshwater yield of  $2 \text{ kg m}^{-2} \text{ day}^{-1}$  to  $3 \text{ kg m}^{-2} \text{ day}^{-1}$  is also consistent with standard performance levels for conventional basin stills reported in literature, such as those reported by Vasava et al. (2023) [5] and Al-Mezeini et al. (2023) [6]. Higher output values, such as the  $4 \text{ kg m}^{-2} \text{ day}^{-1}$  to  $6 \text{ kg m}^{-2} \text{ day}^{-1}$  recorded by Ramzy et al. (2023) [7] and Kumar et al. (2020) [8], typically arise from enhanced systems incorporating reflectors, solar concentrators, fins, or porous media that increase heat absorption. Since the system modelled in this project does not include such augmentation features, the strong alignment between our simulated yields and benchmark values reinforces that the model behaves realistically. Any deviation from enhanced-system performance is therefore attributable to design differences rather than modelling errors.

### 4.2 Irradiance Distribution and Regression Fit

#### Hourly Irradiance Distribution (Fig. 3)

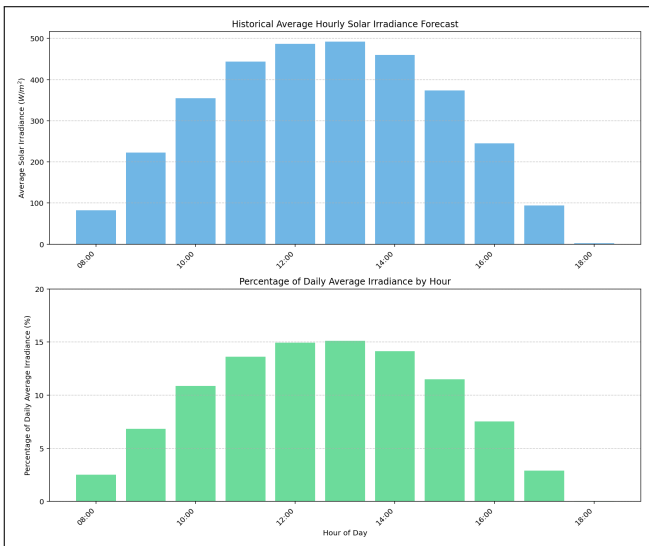


Figure 3: Percentage of daily irradiance occurring at each hour using the irradiance-forcer model.

Figure 3 shows the hourly irradiance fractions produced by the irradiance-forcer model. These values were obtained from a 15-day hourly forecast by averaging the percentage contribution of each hour to the total daily irradiance. The resulting distribution exhibits a smooth, unimodal profile with a peak near solar noon, approaching zero during morning and evening hours. This behaviour is physically consistent with the solar trajectory and confirms that the forcer model can meaningfully convert historical daily totals into hourly inputs for transient simulation.

## Continuous Regression Model (Fig. 4)

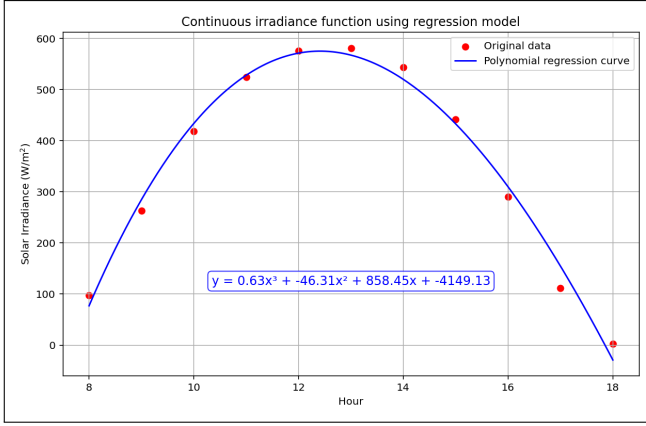


Figure 4: Cubic polynomial regression used to generate a continuous irradiance function.

## 4.3 Thermal Response and Freshwater Output

### Water and Glass Temperature Profiles (Fig. 5)

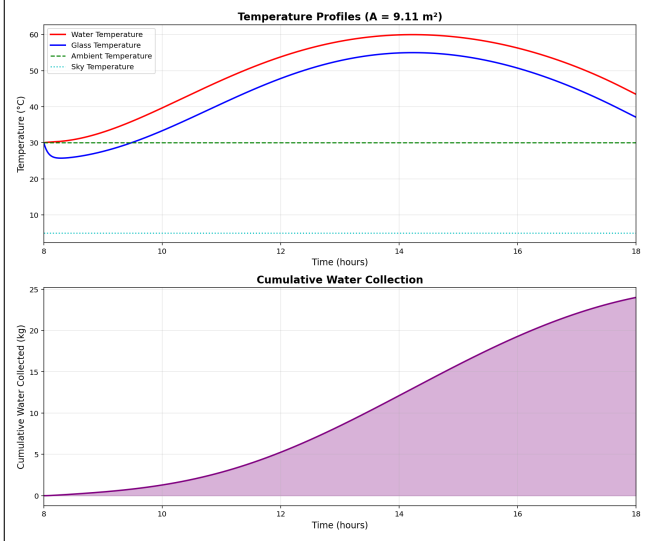


Figure 5: (Top) Water and glass temperature profiles; (Bottom) cumulative freshwater production over 10 hours.

## 4.4 Basin Area Optimisation and Root-Finding

### Water Production vs Basin Area (Fig. 6)

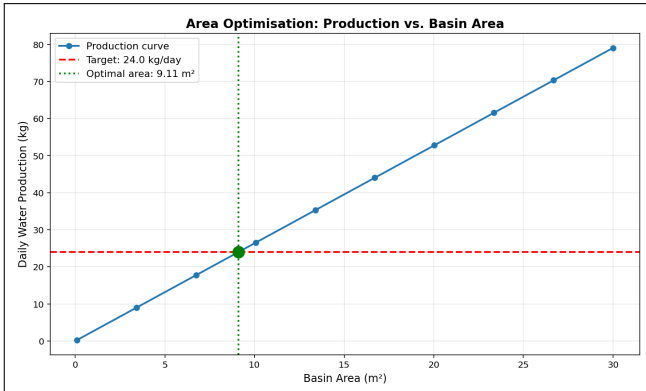


Figure 6: Daily distilled water production as a function of basin area.

Figure 4 shows the cubic regression curve fitted to the reconstructed hourly dataset. The regression model provides a smooth, differentiable function  $G(t)$  suitable for ODE integration. The cubic degree captures the asymmetric daily irradiance pattern without introducing oscillatory artefacts that would arise from higher-order polynomials or spline interpolation. The curve remains positive and monotonic during daylight hours, satisfying physical and numerical sanity checks.

The thermal response presented in Figure 5 aligns strongly with expected solar-still behaviour. Both water and glass begin at ambient temperature, after which the water temperature rises more rapidly due to greater solar energy absorption and lower convective losses. Throughout the day, the water temperature remains consistently  $6^{\circ}\text{C}$ – $10^{\circ}\text{C}$  higher than the glass, satisfying the necessary condition for evaporation and condensation to occur. At no point does  $T_g$  exceed  $T_w$ , confirming correct physical behaviour.

The cumulative freshwater production curve initially increases slowly at sunrise, steepens near midday (when irradiance and the  $T_w - T_g$  driving gradient are largest), and gradually plateaus toward evening. This reflects the underlying physics: evaporation is strongest when both temperatures are elevated and solar input is maximal. The smooth shape of the curve also demonstrates numerical stability within the ODE solver.

Figure 6 illustrates the near-linear relationship between basin area and daily yield. Each data point corresponds to a full run of the ODE simulation at a different basin area. Since evaporation occurs at the water surface, a proportional increase in area leads directly to proportional increases in output, provided boundary conditions remain unchanged. This linearity is consistent with published experimental studies on passive stills.

The observed trend forms the input to the Brent root-finding procedure, where the intersection between the simulated output curve and the required daily potable water demand yields the optimal basin area. Because each function evaluation triggers a full thermal simulation, Brentq's fast and robust bracketing approach is essential for computational efficiency.

## 4.5 Sanity Checks and Physical Plausibility

The following sanity checks were used to validate the physical and numerical correctness of the model:

- **Temperature bounds:** Water temperature remained between ambient and below boiling, and always exceeded the glass temperature, ensuring physically correct evaporation direction.
- **Yield reasonableness:** Predicted daily output of  $2 \text{ kg m}^{-2} \text{ day}^{-1}$  to  $3 \text{ kg m}^{-2} \text{ day}^{-1}$  is consistent with typical passive-sill performance.
- **Regression behaviour:** The polynomial remained smooth and positive with no oscillatory artefacts, ensuring suitable behaviour for ODE integration.
- **Numerical stability:** Temperature and mass-production curves evolved smoothly with no discontinuities across sunrise or sunset, demonstrating appropriate timestep control in RK45.

## 4.6 Summary

The design analysis confirms that the model consistently aligns with empirical expectations for passive solar stills across irradiance reconstruction, thermal dynamics, and freshwater output. Agreement with published literature and successful completion of all sanity checks demonstrate that the model is both physically credible and numerically robust. These validated results form a reliable foundation for the subsequent optimisation of basin area via root-finding.

## 5 Conclusions

Through our system modelling and analysis, we deduced an optimal basin area value of  $9.11\text{m}^2$ . Observing the World Health Organisation paper on water requirements during emergencies [4], and considering the climate of our reference location, we decided that we wanted to accumulate a minimum of 24L of drinkable water per day. This was to ensure that at least 2 households per still (assumed to contain an average of 4 members each) has access to reliable drinking water in times of need, when other drinking water infrastructures may not be available. This basin area achieves our minimum target volume of potable water collected daily whilst keeping the basin area, and thus, the cost of manufacturing to a minimum. In future work, the system could be scaled up to support larger communities. However, meaningful scaling would require improving the efficiency of the current model, so that increases in basin area translate into viable gains in output.

If more time and resources were available, key variables could have been more accurately modelled to increase the realism of results obtained. The limited availability of daily irradiance forecasts meant solar irradiance data only accounted for water output within the autumn months. Through obtaining a larger range of values, future work could assess season variability and develop a more representative understanding of the still's performance throughout the year. Despite this, the key thermodynamic behaviour of the system was captured, with only minor assumptions made to keep the model practical and repeatable.

## References

- [1] Iiss admin. (2023) Less than 0.1% of the earth's water available for human consumption. [Online]. Available: <https://hydrachem.com/less-than-0-1-of-the-earths-water-available-for-human-consumption/>
- [2] World Health Organization. (2025) 1 in 4 people globally still lack access to safe drinking water – who, unicef. [Online]. Available: <https://www.who.int/news-room/detail/26-08-2025-1-in-4-people-globally-still-lack-access-to-safe-drinking-water---who--unicef>
- [3] T. W. B. Group. (2019) Global solar atlas. [Online]. Available: <https://globalsolaratlas.info/download/algeria>
- [4] W. H. Organization. (2013) Technical notes on drinking-water, sanitation and hygiene in emergencies. [Online]. Available: <https://cdn.who.int/media/docs/default-source/wash-documents/who-tn-09-how-much-water-is-needed.pdf>
- [5] V. Vasava, P. Patel, and M. Vyas, “Mathematical modelling of solar still and its comparison analysis with experimental investigation through parametric analysis,” *E3S Web of Conferences*, vol. 398, p. 02006, 2023.
- [6] N. Al-Mezeini, L. Al-Zubaidi, and A. Al-Sulttani, “Design and experimental studies on a single slope solar still for water desalination,” *Water*, vol. 15, no. 4, p. 704, 2023.
- [7] K. Ramzy, A. Salem, and W. El-Maghly, “Performance of a single slope solar still using different porous absorbing materials,” *Environmental Science and Pollution Research*, vol. 30, pp. 12374–12388, 2023.
- [8] A. Kumar, S. Vyas, and D. Nkweetta, “Experimental study of single slope solar still coupled with parabolic trough collector,” *Materials Science for Energy Technologies*, vol. 3, pp. 700–708, 2020.